Dynamics of the Sea Breeze in the Atmospheric Boundary Layer: A Case Study of the Free Convection Regime

SHIH-ANG HSU—*Coastal Studies Institute, Louisiana State University, Baton Rouge, La.*

ABSTRACT—Simultaneous measurements of temperature and wind profiles in the surface boundary layer (below 10-m elevation over a beach and below 100-m elevation over an inland site) under the effect of the sea breeze were made near Fort Walton Beach, Fla. We found that the sea breeze in the atmospheric boundary layer is in the free convection regime and that observed sea-breeze wind and temperature profiles behave according to minus one-third power laws. These experiments also substantiate evidence that the Prandtl-Obukhov-Priestley prediction of the free convection regime is a valid one under appropriate atmospheric conditions.

1. INTRODUCTION

Prandtl (1932), Obukhov (1971), and Priestley (1954) have pointed out independently that the asymptotic state of turbulence in an unstable stratified boundary layer (e.g., the free convection regime in the atmosphere) requires that

$$\frac{\partial \theta}{\partial z} \sim z^{-4/3}$$

and

$$\frac{\partial U}{\partial z} \sim z^{-4/3} \tag{1}$$

where θ is the potential temperature, z is the height coordinate, and U is the magnitude of the horizontal wind.

According to Businger and Yaglom (1971), observations of truly free convection conditions are still scarce, and experimental confirmation of the Prandtl-Obukhov-Priestley predictions has been, until now, somewhat in doubt (Dyer 1965, Elliott 1966, Businger et al. 1971). Businger and Yaglom suggested that a careful study of the free convection case in the atmosphere is still needed. In partial response to this suggestion, a case study of the free convection regime in the atmospheric boundary layer that exists under the sea-breeze condition is given in this paper. Particular emphasis, however, is on the sea-breeze wind profile inasmuch as the temperature fluctuations associated with the free convection regime have been verified by Wyngaard et al. (1971). Some evidence of sea breeze associated with the free convection regime has been given elsewhere (Hsu 1970a).

2. THEORETICAL CONSIDERATIONS

The following derivation for the sea-breeze regime in the surface boundary layer is due in part to McPherson (1970) and is an expanded version of that presented by Estoque (1961).

It is presumed that, in the layer immediately above the surface, the viscous forces acting on a fluid element are much larger than the inertial forces; thus, the horizontal momentum equations and the thermodynamic equation for the layer become

$$\frac{\partial}{\partial z}\left(K \frac{\partial U}{\partial z}\right) = 0 \tag{2}$$

and

$$\frac{\partial}{\partial z}\left(K \frac{\partial \theta}{\partial z}\right) = 0 \tag{3}$$

where K is an eddy exchange coefficient, assumed to be the same for both heat and momentum transfer, U is the magnitude of the horizontal wind, and θ is the potential temperature. If K is known as a function of height, z, the equations can be integrated to obtain U and θ in the boundary layer.

Under conditions of free convection; that is, when the buoyant forces dominate the mechanical forces, the expression of K is, as discussed by Priestley (1959),

$$K = \lambda z^2 \left(\frac{g}{\bar{\theta}}\left|\frac{\partial \theta}{\partial z}\right|\right)^{1/2} \qquad \mathrm{Ri} < -0.03. \tag{4}$$

Here, λ is an empirical constant, g is the acceleration due to gravity, and $\bar{\theta}$ is a layer-mean potential temperature in the layer in which the Richardson number, Ri, is evaluated. Equations (2) and (3) may be written as

$$K \frac{\partial U}{\partial z} = U_*^2 \tag{5}$$

and

$$K \frac{\partial \theta}{\partial z} = \theta_* U_* \tag{6}$$

where U_* and θ_* are termed the "friction velocity" and "friction temperature," respectively. From eq (5) and (6),

FIGURE 1.—Cup anemometer array located in the midforeshore on the coast of the Gulf of Mexico near Fort Walton Beach. A hot-wire anemometer array on the taller offshore mast and a resistance-wire wave gage and an air-sea temperature recording unit on the shorter mast are shown in the background.

we obtain

$$\frac{\partial U}{\partial z}=\frac{U_*}{\theta_*}\frac{\partial \theta}{\partial z} \tag{7}$$

and

$$\frac{\partial \theta}{\partial z}=\frac{\theta_*}{U_*}\frac{\partial U}{\partial z}. \tag{8}$$

For the free convection regime, we use eq (4)-(8) and obtain

$$\frac{\partial U}{\partial z}=\left(\frac{U_*^5\bar{\theta}}{\lambda^2 g|\theta_*|}\right)^{1/3} z^{-4/3} \tag{9}$$

and

$$\frac{\partial \theta}{\partial z}=\left(\frac{U_*^2\theta_*^2\bar{\theta}}{\lambda^2 g}\right)^{1/3} z^{-4/3} \tag{10}$$

Equations (9) and (10) can be integrated between two arbitrary levels, z_1 and z_2, to give

$$U(z_1)-U(z_2)=-3\left(\frac{U_*^5\bar{\theta}}{\lambda^2 g|\theta_*|}\right)^{1/3}(z_1^{-1/3}-z_2^{-1/3}) \tag{11}$$

and

$$\theta(z_1)-\theta(z_2)=-3\left(\frac{U_*^2\theta_*^2\bar{\theta}}{\lambda^2 g}\right)^{1/3}(z_1^{-1/3}-z_2^{-1/3}). \tag{12}$$

Equation (11) can be rewritten as

$$U=3\left(\frac{U_*^5\bar{\theta}}{\lambda^2 g|\theta_*|}\right)^{1/3}(z_0^{-1/3}-z^{-1/3}) \tag{13}$$

in which z_0 is the roughness length [i.e., from eq (11), $U(z_1)=0$ at $z_1=z_0$]. Note that the wind profile [eq (13)] involves no logarithmic height dependency; that is, in the atmospheric free convection regime, the familiar logarithmic wind profile (e.g., Haltiner and Martin 1957) is no longer a valid one.

3. FIELD EXPERIMENTS

Field Sites and Experiments

Two experimental sites, located on the gulf coast near Fort Walton Beach, Fla., were selected. One was the beach site shown in figure 1 (86°43'W, 30°24'N), which has an approximate east-west shoreline orientation. It was used in an earlier study of the local wind system (Hsu 1969). The experiment discussed in this study was performed during May 1970. It was designed to measure the wind and temperature profiles in the surface boundary layer, as shown in eq (11) and (12), respectively.
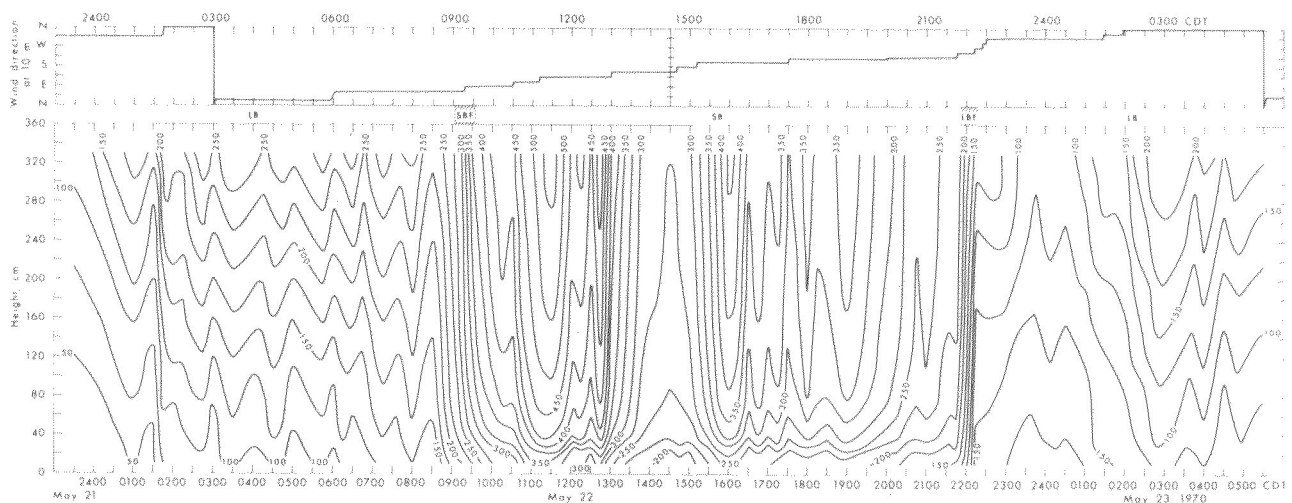

FIGURE 2.—Microstructure of the land breeze and sea breeze in the surface boundary layer on the beach face near Fort Walton Beach. LB stands for land breeze, SBF for sea-breeze front, SB for sea breeze, LBF for land-breeze front, and the numbers (such as 100, 150, 200, etc.) for U (cm/s).
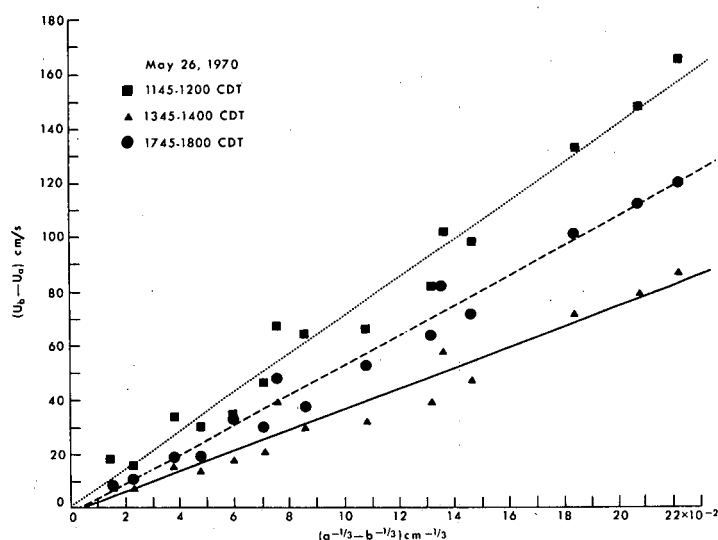
FIGURE 3.—Examples of the relationship between sea-breeze wind and elevation [(cf. eq (15a), (15b), (15c)] over the beach face near Fort Walton Beach.

Temperature and wind profiles in the atmospheric boundary layer below 100 m were based on measurements made from a meteorological tower at Eglin Air Force Base, Fla., which was about 10 km from the beach site. Measurements were made at four levels, approximately 2, 18, 54, and up to 100 m for the vertical temperature and at 4, 18, 54, and 100 m for the wind.

Instrumentation

The main instrument used for this study was a portable Thornthwaite Wind Profile Register System (C. W. Thornthwaite Associates, Model 106)[1] with six-unit, three-cup, fast-response anemometers mounted 20, 40, 80, 160, 240, and 320 cm above the beach surface (fig. 1). The instrumentation and wind data reduction procedures have been described elsewhere (Hsu 1971a).

Temperatures were measured at 170, 360, and 550 cm above a grass-free berm surface by three identical recording hygrometry systems (Taylor Instrument Company, Series 76J, having readings within ± 1 percent of any given chart range). The sensors were mounted on a 10-m meteorological tower. An all-purpose wind-recording system (Science Associates Inc., No. 162) at the 10-m level above the surface made wind speed and direction measurements at the reference level.

Detailed information about the meteorological tower facility at Eglin AFB, along with related instrumentation and data processing procedures, will not be covered here because of military regulations.

4. STRUCTURE OF THE SEA BREEZE BELOW 10 m OVER THE BEACH SURFACE

Before we go into the studies of sea-breeze wind profile, some understanding of the microstructure and characteristics of this wind system may be helpful. The micro-

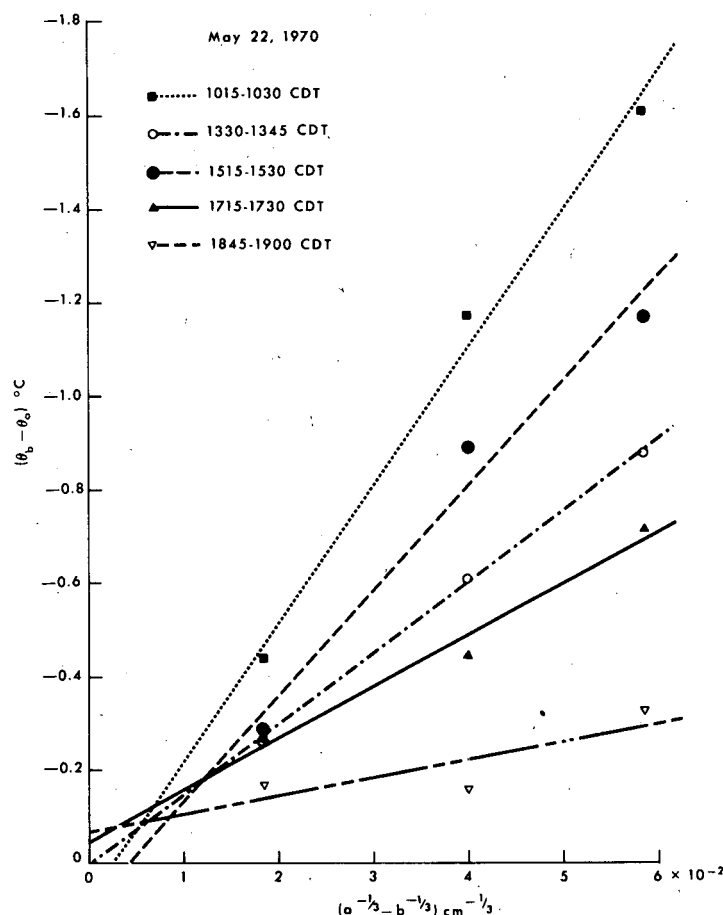[1] Mention of a commercial product does not constitute endorsement.

FIGURE 4.—Examples of the relationship between sea-breeze temperature and elevation [obtained from a set of equations parallel with eq (15a), (15b), (15c) for the temperature profiles as listed in table 2] over the grass-free berm surface near Fort Walton Beach.

structure of the sea breeze in the surface boundary layer should be composed of at least the following major characteristics. After the passage of the sea-breeze front in the morning, wind direction should shift clockwise in the Northern Hemisphere (Coriolis effect); that is, from a land breeze to a sea breeze, and the wind speed should increase. Meanwhile, cooler temperatures should prevail. Toward evening, the wind should become weaker because of the diminishing difference in air temperature between land and sea until the onset of the land-breeze front. This sequence is shown in figure 2. Some temperature characteristics associated with the sea-breeze front in the area of concern have been studied and presented elsewhere (Hsu 1969). Further evidence on the temperature profiles in the surface boundary layer is given later in table 2 (cf. fig. 4).

Since our immediate concern is to examine the validity of eq (11) and (12) under sea-breeze conditions, let us proceed as follows. First, eq (11) can be written as

$$U(z_2)-U(z_1)=3\left(\frac{U_*^5\bar{\theta}}{\lambda^2 g|\theta_*|}\right)^{1/3}(z_1^{-1/3}-z_2^{-1/3}) \quad (14)$$

TABLE 1.—*Sea-breeze wind (cm/s) profiles in the surface boundary layer on the beach face near Fort Walton Beach, Fla., on May 22, 1970*

15-min ending time	Height						Least-squares values	
	20 cm	40 cm	80 cm	160 cm	240 cm	320 cm	Correlation coefficient r	y axis intercept a_0
(CDT)	(cm/s)	(cm/s)	(cm/s)	(cm/s)	(cm/s)	(cm/s)		(cm/s)
0800*	139	154	168	196	226	267	0.61	25.1
15*	152	169	185	213	248	276	.69	21.8
30*	138	149	164	189	216	244	.66	19.7
45*	130	144	158	181	200	227	.73	15.6
0900*	160	176	192	209	223	242	.86	9.6
15†	190	211	227	247	254	262	.98	2.6
30†	209	235	258	282	291	300	.99	2.6
45†	240	272	303	341	361	377	.96	9.1
1000	266	304	336	367	382	395	.99	4.1
15	282	323	360	393	410	426	.99	5.1
30	297	340	380	416	431	447	.99	4.1
45	300	346	379	406	421	435	.99	2.2
1100	337	389	424	455	466	480	.99	-0.0
15	354	407	443	472	484	499	.99	0.1
30	369	428	465	493	507	523	.99	-0.2
45	374	431	468	501	518	535	.99	2.4
1200	347	413	448	478	494	511	.99	0.1
15	322	382	417	444	456	471	.99	-1.4
30	312	381	421	447	462	477	.99	-2.6
45	298	362	394	419	434	448	.98	-1.4
1300	326	395	431	460	472	488	.98	-2.6
15	270	324	353	374	385	398	.98	-1.6
30	250	301	326	345	352	361	.98	-3.8
45	233	279	300	316	324	332	.97	-2.8
1400	213	252	270	284	291	299	.98	-1.8
15	205	242	261	275	282	290	.98	-1.6
30	202	240	258	273	280	287	.98	-1.9
45	190	231	249	262	267	275	.98	-3.1
1500	201	238	256	271	278	286	.98	-1.3
15	198	240	260	277	285	294	.98	-1.5
30	216	263	290	307	317	326	.98	-2.3
45	230	280	310	330	342	352	.99	-1.7
1600	265	319	355	374	386	396	.99	-3.2
15	276	335	374	401	414	428	.99	-1.5
30	266	318	358	383	396	406	.99	-2.0
45	230	280	312	332	345	355	.99	-1.5
1700	246	300	332	351	363	373	.98	-2.8
15	230	277	313	332	343	352	.99	-2.5
30	237	291	323	342	351	360	.98	-4.2
45	213	259	291	307	316	322	.98	-4.2
1800	216	264	298	317	328	336	.99	-2.9
15	232	286	326	346	356	364	.98	-4.8
30	222	270	302	320	327	335	.98	-4.3
45	216	265	301	321	332	340	.99	-3.1
1900	227	277	314	335	345	353	.99	-3.7
15	237	289	328	349	361	369	.99	-3.5
30	224	277	314	335	345	352	.99	-4.6
45	217	265	301	321	332	339	.99	-3.3
2000	204	252	285	302	310	315	.98	-5.2
15	200	247	279	296	305	311	.98	-4.2
30	193	238	268	282	291	296	.98	-4.4
45	176	215	243	257	264	268	.98	-4.2
2100	166	205	231	245	251	256	.98	-4.0
15	174	214	242	255	262	267	.98	-4.2
30	167	204	230	244	249	254	.98	-4.0
45	159	192	216	228	233	237	.98	-3.7
2200	163	190	212	231	236	241	.99	-1.0
15†	111	127	143	163	174	187	.92	6.8
30†	44	48	59	74	88	135	.40	21.9

*For reference only: land-breeze regime
†For reference only: sea-breeze or land-breeze fronts

TABLE 2.—*Sea-breeze temperature (°C) profiles in the surface boundary layer on a grass-free berm surface near Fort Walton Beach, Fla., on May 22, 1970*

15-min. ending time	Height			Least-squares values	
	170 cm	360 cm	550 cm	Correlation coefficient r	y axis intercept a_0
(CDT)	(°C)	(°C)	(°C)		(°C)
0900	27.22	26.22	26.11	0.93	-0.25
15	28.00	26.94	26.44	1.00	.01
30	27.61	26.83	25.89	0.75	.41
45	27.28	26.50	25.83	.91	.22
1000	27.28	26.44	25.72	.91	.24
15	27.22	26.39	25.67	.90	.24
30	27.50	26.33	25.89	1.00	- .07
45	27.50	26.56	25.78	0.92	.25
1100	27.22	26.22	25.78	1.00	- .02
15	26.94	26.17	25.72	0.99	.07
30	26.67	26.11	25.56	.85	.21
45	26.61	26.11	25.56	.80	.23
1200	26.67	26.11	25.61	.89	.17
15	26.67	26.11	25.56	.85	.21
30	26.67	26.06	25.61	.95	.12
45	26.72	26.11	25.67	.96	.11
1300	26.89	26.17	25.72	.98	.08
15	26.89	26.28	25.83	.95	.12
30	26.94	26.22	26.00	.98	- .08
45	26.94	26.33	26.06	1.00	- .01
1400	27.11	26.56	26.11	0.92	.14
15	27.11	26.61	26.11	.84	.19
30	26.94	26.61	26.11	.62	.25
45	27.00	26.61	26.11	.71	.23
1500	27.44	26.56	26.33	.97	- .13
15	27.67	26.67	26.61	.91	- .29
30	27.78	26.89	26.61	.99	- .09
45	27.44	26.78	26.17	.88	.22
1600	27.66	26.56	26.11	.97	.10
15	27.17	26.39	26.11	.99	- .06
30	27.22	26.50	26.22	1.00	- .04
45	26.94	26.61	26.06	0.56	.28
1700	26.56	26.33	25.72	.33	.36
15	26.33	26.06	25.61	.56	.23
30	26.39	25.94	25.67	.99	.04
45	26.39	26.06	25.67	.76	.17
1800	26.22	26.06	25.72	.43	.19
15	26.11	26.06	25.67	.76	.26
30	26.11	25.94	25.61	.48	.18
45	26.06	25.89	25.56	.48	.18
1900	25.83	25.67	25.50	.82	.07
15	25.67	25.61	25.44	.31	.10
30	25.50	25.56	25.22	-.18	.26
45	25.39	25.50	25.17	-.28	.27
2000	25.22	25.44	25.06	-.40	.34
15	25.06	25.28	25.00	-.48	.27
30	25.00	25.22	25.00	-.54	.23
45	25.00	25.11	25.00	-.54	.11
2100	25.00	25.11	25.00	-.54	.11
15	25.00	25.11	25.00	-.54	.11
30	24.94	25.06	25.00	-.69	.08
45	24.89	25.06	25.00	-.74	.10
2200	24.67	25.06	25.00	-.79	.01

or, between any two heights $a(=z_1)$ and $b(=z_2)$, we have

$$U_b-U_a=3\left(\frac{U_*^5\bar\theta}{\lambda^2 g|\theta_*|}\right)^{1/3}(a^{-1/3}-b^{-1/3}). \tag{15a}$$

This may be written

$$y=a_0+a_1 x \tag{15b}$$

where

$$y=U_b-U_a,$$
$$a_0=0,$$
$$a_1=3\left(\frac{U_*^5\bar\theta}{\lambda^2 g|\theta_*|}\right)^{1/3},$$

and

$$x=a^{-1/3}-b^{-1/3}. \tag{15c}$$

We plot the observations for each run in the form y against x, plotting one point for each available pair of heights. Equation (15b) shows that, if the data do follow the free convection form, the points lie on a straight line. This method is similar to that used by Webb (1970).

TABLE 3.—*Sea-breeze temperature (°F) profiles at Eglin AFB, Fla., near Fort Walton Beach on May 21, 1969*

15-min ending time	Height				Least-squares values	
	6 ft	54 ft	162 ft	300 ft	Correlation coefficient r	y axis intercept a_0
(CDT)	(°F)	(°F)	(°F)	(°F)		(°F)
1000	85.31	84.07	83.49	83.15	0.97	0.24
15	87.19	85.11	84.05	84.06	.98	.05
30	87.29	85.11	84.04	84.29	.97	−.12
45	87.30	85.20	84.83	84.97	.98	−.37
1100	88.18	85.58	84.87	85.16	.98	−.41
15	87.32	85.76	85.03	84.79	.99	.16
30	88.64	86.58	85.72	85.57	.99	.07
45	88.95	86.98	86.07	86.08	.98	.01
1200	89.14	87.16	86.21	85.86	.98	.26
15	90.11	87.81	86.58	86.44	.98	.19
30	89.23	87.22	86.61	86.49	1.00	−.06
45	88.94	86.95	86.48	86.19	1.00	−.01
1300	90.52	88.38	87.35	86.85	0.98	.36
15	91.42	88.72	87.47	87.45	.98	.03
30	91.44	88.36	87.50	87.66	.99	−.35
45	91.71	88.82	87.97	88.04	.99	−.26
1400	91.93	89.59	88.64	88.79	.98	−.15
15	91.71	89.90	88.96	88.56	.98	.37
30	91.83	89.37	88.60	88.45	1.00	−.06
45	91.68	89.14	88.58	88.49	0.99	−.22
1500	89.95	88.53	88.20	87.51	.93	.31
15	92.27	90.68	89.88	89.31	.95	.42
30	90.01	88.83	88.45	87.81	.91	.35
45	91.98	90.39	89.78	89.22	.97	.32
1600	91.73	89.28	88.67	88.83	.98	−.19
15	91.60	89.82	89.32	88.90	.99	.13
30	91.04	89.47	89.10	88.74	.99	.13
45	90.37	89.36	89.01	88.26	.99	.08
1700	89.65	88.75	88.55	87.97	.82	.45
15	89.57	88.66	88.50	87.94	.86	.29
30	88.84	88.16	88.10	87.47	.87	.25
45	88.12	87.61	87.58	87.00	.70	.30
1800	87.06	86.74	86.81	86.32	.37	.22

Equations (15b) and (15c) have also been obtained by the least-squares technique. This method of data analysis and the results are illustrated in figure 3. Tables 1 and 4 give the least-squares values of each correlation coefficient, r, as well as the y-axis intercept, a_0.

Similar analyses were made for temperature profiles under sea-breeze conditions whenever wind profiles were measured. Examples are given in figure 4 and tables 2 and 3.

Figure 5 shows some of the measured sea-breeze wind profiles. Note that, for brevity, only those profiles that do not overlap are plotted in the figure. For the entire diurnal variation of the profile, however, table 1 should be consulted. Also included in figure 5 is an example of the predicted sea-breeze wind profile using eq (13) and those parameters listed in the figure. The choice of the value of $\lambda = 1$ is based on the findings by Priestley (1959), Deardorff and Willis (1967), and Dyer (1967).

The shape of the predicted sea-breeze wind profile is in excellent agreement with those observed (fig. 5). In fact, table 1 gives considerable evidence that, in the whole sea-breeze range from 1000 to 2200 CDT, the least-squares values of each correlation coefficient, r, is greater than 0.96 and that -5.2 cm/s$<a_0<5.2$ cm/s, which is within the experimental error. Examples of the sea-breeze temperature profiles are listed in table 2. Because temperatures were measured at only three levels, the correlation coefficients for these profiles were naturally less than those for the wind profiles. Nevertheless, in the major sea-
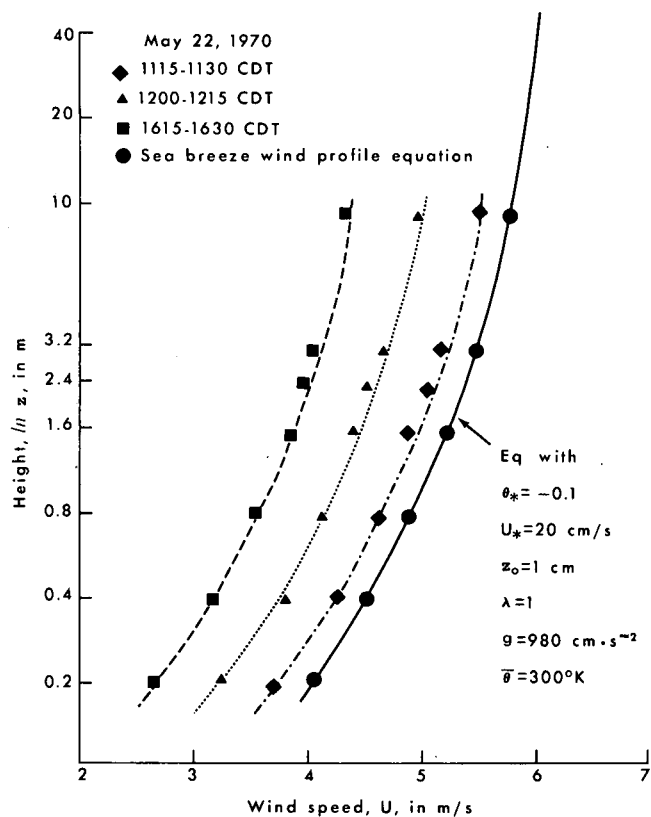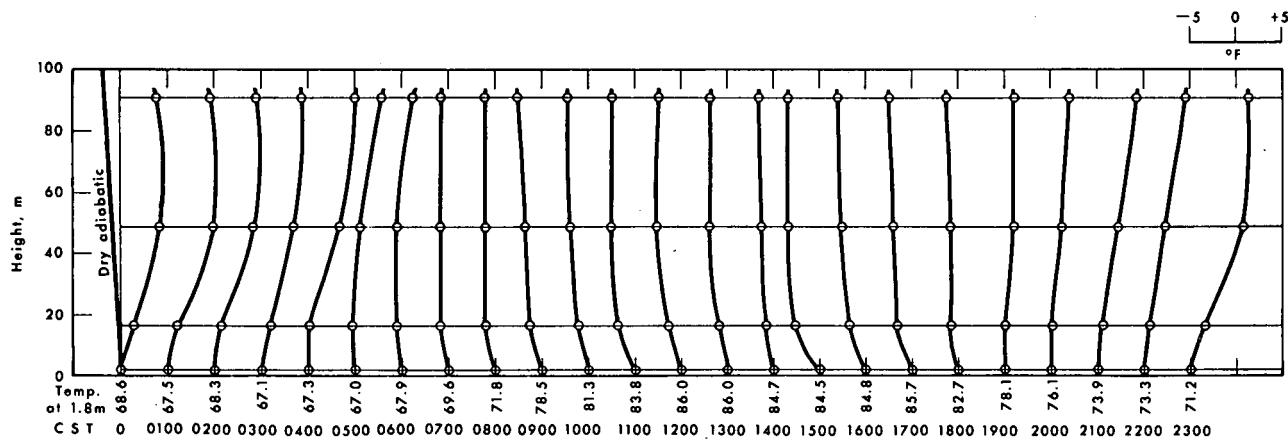

FIGURE 5.—Examples of measured sea-breeze wind profiles in the surface boundary layer near Fort Walton Beach. Included also is the predicted sea-breeze wind profile equation with parameters from eq (13) specified in the figure.

TABLE 4.—*Sea-breeze wind (kt) profiles at Eglin AFB, Fla., near Fort Walton Beach on May 21, 1969*

15-min ending time	Height				Least-squares values	
	12 ft	54 ft	162 ft	300 ft	Correlation coefficient r	y axis intercept a_0
(CDT)	(kt)	(kt)	(kt)	(kt)		(kt)
1000	4.79	5.15	5.24	6.31	0.21	0.59
15	7.90	9.45	8.99	8.60	.70	−.81
30	6.28	7.35	7.91	8.48	.95	.24
45	6.63	8.28	8.88	9.13	.99	−.10
1100	7.88	9.03	9.55	9.59	.99	−.12
15	4.19	4.90	6.58	7.23	.69	.74
30	6.68	8.39	8.68	8.56	.93	−.48
45	6.80	8.29	8.83	10.23	.78	.63
1200	5.76	6.52	7.57	8.61	.66	.77
15	7.32	8.80	9.50	9.76	1.00	−.02
30	8.47	10.48	10.77	11.04	0.95	−.29
45	6.67	7.75	8.48	9.46	.82	.54
1300	7.83	9.32	9.25	9.39	.88	−.34
15	8.59	10.60	11.13	11.31	.98	−.27
30	7.91	8.82	9.32	9.14	.94	−.20
45	8.61	9.96	10.34	10.26	.96	−.29
1400	7.83	9.35	10.30	10.59	.99	.07
15	6.75	7.86	8.35	8.76	.99	.11
30	5.42	6.39	6.64	8.00	.56	.65
45	8.30	9.75	10.53	10.99	.99	.14
1500	7.49	9.13	9.50	9.78	.97	−.19
15	8.05	9.28	9.74	10.09	.99	.03
30	8.20	10.11	11.14	10.98	.97	−.34
45	9.29	11.46	12.23	12.66	1.00	−.08
1600	8.37	10.07	10.57	10.91	0.99	−.09
15	11.45	13.86	13.80	13.70	.87	−.74
30	9.06	11.35	12.23	12.35	.99	−.27
45	9.90	12.39	13.19	13.91	.99	−.02
1700	8.50	10.51	10.76	11.42	.94	−.06
15	9.11	11.28	12.44	12.88	1.00	−.05
30	7.36	9.24	10.08	10.82	0.98	.21
45	6.64	8.26	8.63	9.68	.88	.32
1800	5.81	6.98	8.54	9.71	.76	.90

FIGURE 6.—Diurnal variation of temperature between 1.8 and 90.9 m at Eglin AFB, near Fort Walton Beach, May 20, 1969.

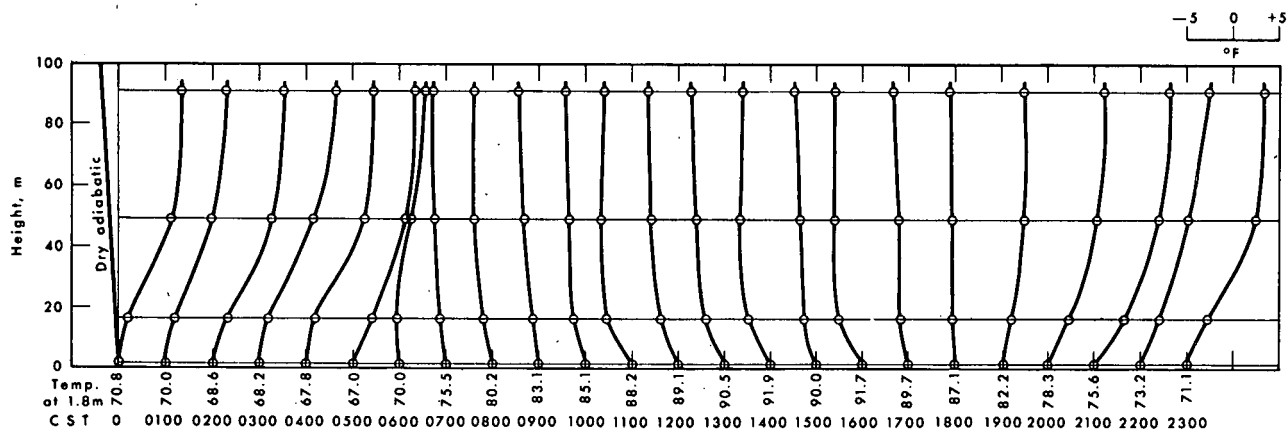| Temp. at 1.8m	68.6	67.5	68.3	67.1	67.3	67.0	67.9	69.6	71.8	78.5	81.3	83.8	86.0	86.0	84.7	84.5	84.8	85.7	82.7	78.1	76.1	73.9	73.3	71.2
CST	0	0100	0200	0300	0400	0500	0600	0700	0800	0900	1000	1100	1200	1300	1400	1500	1600	1700	1800	1900	2000	2100	2200	2300

FIGURE 7.—Same as figure 6 for May 21, 1969.

Temp. at 1.8m	70.8	70.0	68.6	68.2	67.0	67.0	70.0	75.5	80.2	83.1	85.1	88.2	89.1	90.5	91.9	90.0	91.7	89.7	87.1	82.2	78.3	75.6	73.2	71.1
CST	0	0100	0200	0300	0400	0500	0600	0700	0800	0900	1000	1100	1200	1300	1400	1500	1600	1700	1800	1900	2000	2100	2200	2300

breeze regime from 0900 to 1900 CDT, we obtained values for r that are highly significant and values for a_0 that are within the acceptable experimental error. In other words, these observations verify that the sea breeze is in the atmospheric free convection regime and that its wind and temperature profiles in the surface boundary layer can be represented by eq (11) and (12), respectively.

5. SEA-BREEZE TEMPERATURE AND WIND PROFILES BELOW 100 m ON AN INLAND SITE

To further support the results given in section 4, we present independent measurements of sea-breeze temperature and wind profiles below 100 m on an inland site. As mentioned previously, these profiles are based on measurements made from a meteorological tower at Eglin AFB, near Fort Walton Beach. Because land and sea breezes, as well as their fronts near the surface, were observed on May 20 and 21, 1969 (Hsu 1969), these 2 days were selected for this study.

Figures 6 and 7 show the hourly variation of the temperature profile between 1.8 and 90.9 m for May 20 and 21, respectively. For reference, times of sunrise and sunset for these 2 days were approximately 0504 and 1849 CST, respectively. Since the lapse rate, γ, of the actual temperature, T, is defined as the rate of T decrease with height, z, (i.e., $\gamma = -dT/dz$) and since the dry adiabatic lapse rate, γ_d, is 0.98°C/100 m (or 5.4°F/1,000 ft), the
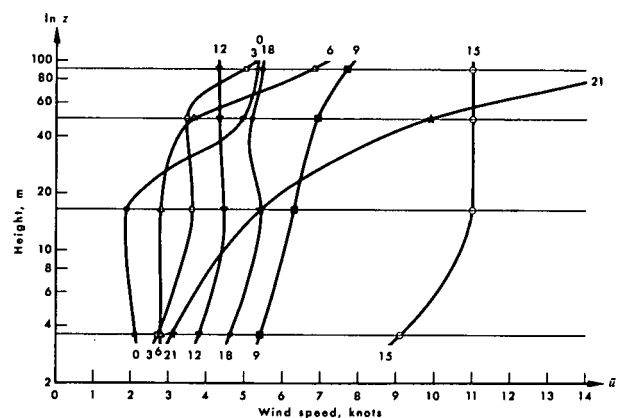
FIGURE 8.—Wind profiles between 3.6 and 90.9 m at Eglin AFB May 20, 1969.

stability criteria for the unsaturated air may be written as (e.g., Haltiner and Martin 1957)

$$\gamma > \gamma_d \quad \text{unstable,}$$
$$\gamma = \gamma_d \quad \text{neutral,}$$
and
$$\gamma < \gamma_d \quad \text{stable.}$$

Comparing the hourly temperature profiles with the dry adiabatic lapse rate shown on the left of figures 6 and 7, we see that, in general, conditions are stable at night and
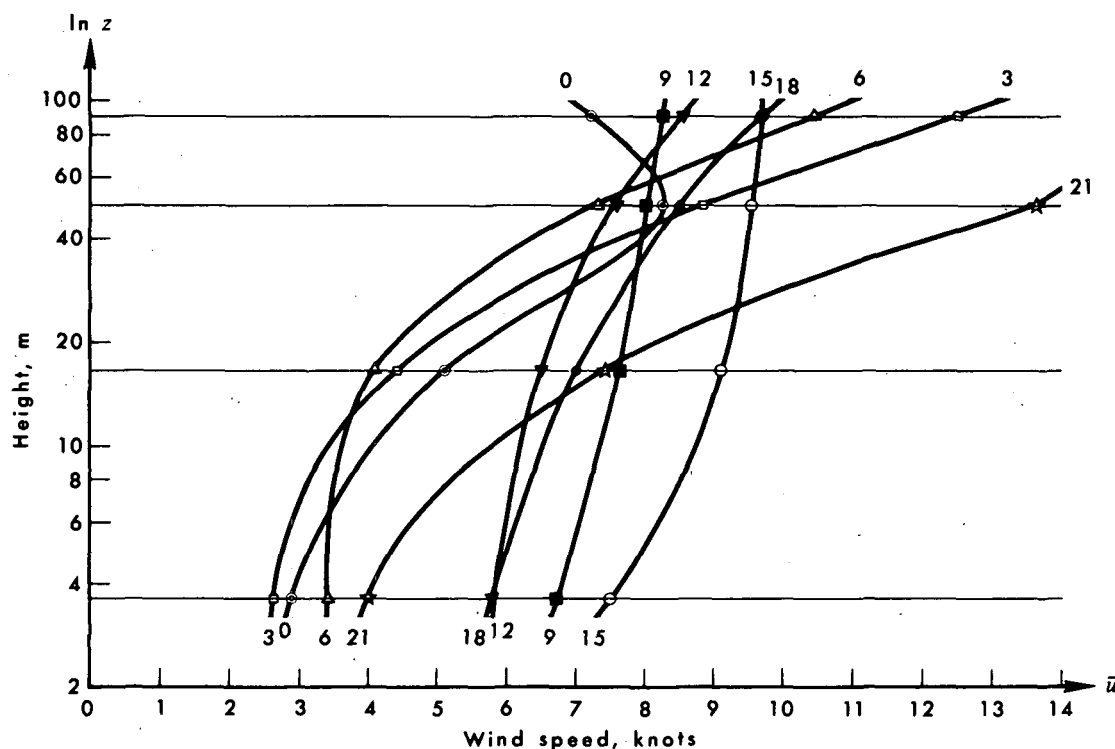
FIGURE 9.—Same as figure 8 for May 21, 1969.

unstable during the day over the coastal zone. Sea-breeze temperature profiles in the atmospheric boundary layer, which is also in the free convection regime, are given in table 3.

From Figures 6 and 7, the following features are also noted (cf. Sutton 1953, pp. 190–192):

1. During the day, temperature decreases with height, rapidly in the lowest layers and more slowly at greater heights. Furthermore, the cooling effect of the sea breeze tends to modify the profile to a near-isothermal one, even though the lowest layers may still be in the superadiabatic lapse rate situation because of the surface condition (cf. Hsu 1969).

2. At night, temperature increases with height (i.e., the inversion case) with the greatest gradient in the middle layers instead of in the lowest layers. In other words, a pool of cold air forms in the lowest layers during the night. The cool pool phenomenon associated with land-breeze genesis on the coast has been studied in more detail by Hsu (1970b).

According to Sutton (1953, p. 230), the normal diurnal variation of the coastal wind tends to be masked by land breezes and sea breezes. The diurnal variations of wind speed between 3.6 and 90.9 m for May 20 and 21 under the land- and sea-breeze conditions are shown in figures 8 and 9, respectively. Note that the wind profiles are plotted on semilogarithmic paper so that a straight line may be fitted for the neutral stability; that is, for the law of logarithmic wind profile (e.g., Haltiner and Martin 1957). For the sake of clarity, profiles are plotted for every 3 hr instead of for each hour.

Figures 8 and 9 clearly show that the wind profile is concave either upward or downward except around mid-morning (0900 LST) when the transitional period occurs between land breeze and sea breeze. (See figs. 1 and 2 of Hsu 1969.) Caution should be used, therefore, in applying

the law of logarithmic wind profile in the coastal zone, at least under land- and sea-breeze conditions. Furthermore, particular attention should be given to the afternoon sea-breeze wind profile (1500 CST) in figures 8 and 9. Excellent agreement can be seen between the shapes of these profiles with that predicted by eq (13), as shown in figure 5, particularly around 1500 CST on May 21, 1969 (fig. 9). Further description of the sea-breeze wind profile in the atmospheric boundary layer is given in table 4. The typical nighttime land-breeze profile (2100 CST) is also shown in figures 8 and 9.

6. CONCLUDING REMARKS

Expressions for the wind and temperature profiles [eq (11) and (12)] are derived for the sea-breeze regime in the surface boundary layer, assuming that free convection conditions exist. A case study of the free convection regime is made to determine the validity of these equations. The results of this study verify that the sea breeze is in the atmospheric free convection regime and that its wind and temperature profiles in the surface boundary layer can be represented by the equations.

Murray (1972) has shown that the sea breeze is effective in generating waves and currents, which in turn transport sediments in the littoral environment. Eolian sand transport (Inman et al. 1966, Hsu 1971b) and air pollution (Neiburger 1969) in the coastal zone are also closely controlled by this localized wind system. We recommend, therefore, that similar experiments be conducted for both sea- and land-breeze conditions in other geographical regions (Defant 1951, Baralt and Brown 1965) using more detailed measurements such as those of Wyngaard et al. (1971) and Hembree (1971).

REFERENCES

Baralt, Gisela L., and Brown, Rodger A., "The Land and Sea Breezes: An Annotated Bibliography," *Final Report*, 1960–65, Contract No. AF 19(604)–7259, Department of the Geophysical Sciences, University of Chicago, Ill. Feb. **1965**, 61 pp.

Businger, J. A., Wyngaard, J. C., Izumi, Y., and Bradley, E. F., "Flux Profile Relationships in the Atmospheric Surface Layer," *Journal of the Atmospheric Sciences*, Vol. 28, No. 2, Mar. **1971**, pp. 181–189.

Businger, J. A., and Yaglom, A. M., "Introduction to Obukhov's Paper on 'Turbulence in an Atmosphere with a Non-uniform Temperature,'" *Boundary-Layer Meteorology*, Vol. 2, No. 1, Dordrecht, Netherlands, Sept. **1971**, pp. 3–6.

Deardorff, J. W., and Willis, G. E., "The Free-convection Temperature Profile," *Quarterly Journal of the Royal Meteorological Society*, Vol. 93, No. 396, London, England, Apr. **1967**, pp. 166–175.

Defant, Friedrich, "Local Winds," *Compendium of Meteorology*, American Meteorological Society, **1951**, pp. 655–672.

Dyer, A. J., "The Flux-Gradient Relation for Turbulent Heat Transfer in the Lower Atmosphere," *Quarterly Journal of the Royal Meteorological Society*, Vol. 91, No. 388, London, England, Apr. **1965**, pp. 151–157.

Dyer, A. J., "The Turbulent Transport of Heat and Water Vapour in an Unstable Atmosphere," *Quarterly Journal of the Royal Meteorological Society*, Vol. 93, No. 398, London, England, Oct. **1967**, pp. 501–508.

Elliott, William P., "Daytime Temperature Profiles," *Journal of the Atmospheric Sciences*, Vol. 23, No. 6, Nov. **1966**, pp. 678–681.

Estoque, M. A., "A Theoretical Investigation of the Sea Breeze," *Quarterly Journal of the Royal Meteorological Society*, London, England, Vol. 87, No. 372, Apr. **1961**, pp. 136–146.

Haltiner, George J., and Martin, Frank L., *Dynamical and Physical Meteorology*, McGraw-Hill, New York, **1957**, 470 pp.

Hembree, L. A., Jr., "Turbulent Fluxes and Associated Spectra in a Sea Breeze Boundary Layer," *Final Report* No. 29, Atmospheric Science Group, University of Texas, Austin, **1971**, 90 pp.

Hsu, Shih-Ang, "Land and Sea-breeze Fronts near 50 cm on the Gulf Coast," *Bulletin of the American Meteorological Society*, Vol. 50, No. 11, Nov. **1969**, pp. 880–882.

Hsu, Shih-Ang, "The Shear Stress of Sea Breeze on a Swash Zone," *Proceedings of the 12th Coastal Engineering Conference, September 13–18, 1970, Washington, D.C.*, Vol. 1, American Society of Civil Engineers, New York, N.Y., Sept. **1970**a, pp. 243–255.

Hsu, Shih-Ang, "Coastal Air-circulation System: Observations and Empirical Model," *Monthly Weather Review*, Vol. 98, No. 7, July **1970**b, pp. 487–509.

Hsu, Shih-Ang, "Measurement of Shear Stress and Roughness Length on a Beach," *Journal of Geophysical Research*, Vol. 76, No. 12, Apr. 20, **1971**a, pp. 2880–2885.

Hsu, Shih-Ang, "Wind Stress Criteria in Eolian Sand Transport," *Journal of Geophysical Research*, Vol. 76, No. 36, Dec. 20, **1971**b, pp. 8684–8686.

Inman, D. L., Ewing, G. C., and Corliss, J. B., "Coastal Sand Dunes of Guerrero Negro, Baja California, Mexico," *Geological Society of America Bulletin*, Vol. 77, No. 8, Aug. **1966**, pp. 787–802.

McPherson, Ronald D., "A Numerical Study of the Effect of a Coastal Irregularity on the Sea Breeze," *Journal of Applied Meteorology*, Vol. 9, No. 5, Oct. **1970**, pp. 767–777.

Murray, Stephen P., "Trajectories of Wind-driven Inshore Currents," Abstract in *Transactions, American Geophysical Union*, Vol. 53, No. 4, Apr. **1972**, pp. 396–397.

Neiburger, Morris, "The Role of Meteorology in the Study and Control of Air Pollution," *Bulletin of the American Meteorological Society*, Vol. 50, No. 12, Dec. **1969**, pp. 957–965.

Obukhov, A. M., "Turbulence in an Atmosphere With a Non-uniform Temperature," *Boundary-Layer Meteorology*, Vol. 2, No. 1, Dordrecht, Netherlands, Sept. **1971**, pp. 7–29.

Prandtl, Ludwig Von, "Meteorologische Anwendungen der Strömungslehre," (Meteorological Applications of Hydrodynamics), *Beiträge zur Physik der freien Atmosphäre, Bjerknes-Festschrift*, Vol. 19, Braunschweig, Germany, **1932**, pp. 188–202.

Priestley, C. H. B., "Convection From a Large Horizontal Surface," *Australian Journal of Physics*, Vol. 7, No. 1, Melbourne, Mar. **1954**, pp. 176–201.

Priestley, C. H. B., *Turbulent Transfer in the Lower Atmosphere*, University of Chicago Press, Ill., **1959**, 130 pp.

Sutton, O. G., *Micrometeorology*, McGraw-Hill Inc., New York, N.Y., **1953**, 333 pp.

Webb, E. K., "Profile Relationships: The Log-linear Range, and Extension to Strong Stability," *Quarterly Journal of the Royal Meteorological Society*, Vol. 96, No. 407, London, England, Jan. **1970**, pp. 67–90.

Wyngaard, J. C., Cote, O. R., and Izumi, Y., "Local Free Convection, Similarity, and the Budgets of Shear Stress and Heat Flux," *Journal of the Atmospheric Sciences*, Vol. 28, No. 7, Oct. **1971**, pp. 1171–1182.